JACS
JOURNAL OF THE AMERICAN CHEMICAL SOCIETY

Article

pubs.acs.org/JACS

Reduction-Triggered Self-Assembly of Nanoscale Molybdenum Oxide Molecular Clusters

Panchao Yin,[*,†,⊥] Bin Wu,[‡,⊥] Tao Li,[⊗] Peter V. Bonnesen,[§] Kunlun Hong,[§] Soenke Seifert,[⊗] Lionel Porcar,[∥] Changwoo Do,[#] and Jong Kahk Keum[†,§]

[†]Chemical and Engineering Materials Division, Neutron Sciences Directorate, Oak Ridge National Laboratory, Oak Ridge, Tennessee 37831, United States

[‡]Department of Physics and Astronomy, University of Tennessee, Knoxville, Tennessee 37996, United States

[⊥]Shull Wollan Center, Neutron Sciences Directorate, Oak Ridge National Laboratory, Oak Ridge, Tennessee 37831, United States

[⊗]X-Ray Science Division, Advanced Photon Source, Argonne National Laboratory, Argonne, Illinois 60439, United States

[§]Center for Nanophase Materials Sciences, Oak Ridge National Laboratory, Oak Ridge, Tennessee 37831, United States

[∥]Institute Max Von Laue Paul Langevin, F-38042 Grenoble 9, France

[#]Biology and Soft Matter Division, Neutron Sciences Directorate, Oak Ridge National Laboratory, Oak Ridge, Tennessee 37831, United States

Supporting Information

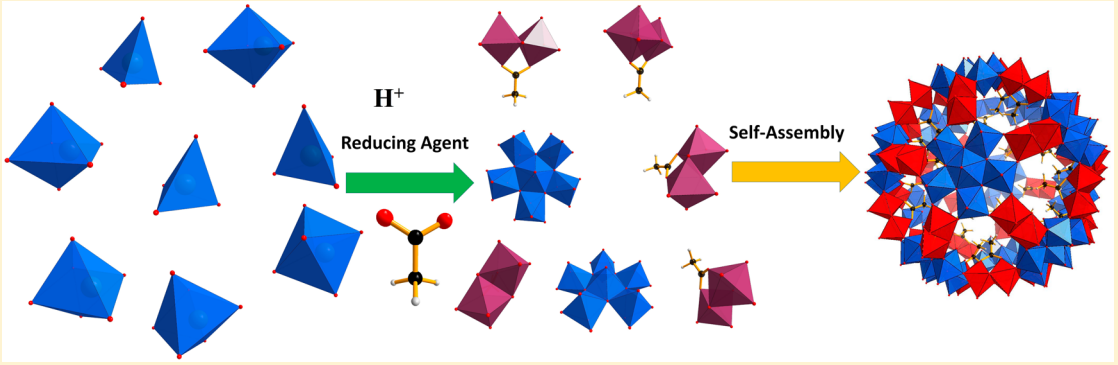

ABSTRACT: Understanding the formation mechanism of giant molecular clusters is essential for rational design and synthesis of cluster-based nanomaterials with required morphologies and functionalities. Here, typical synthetic reactions of a 2.9 nm spherical molybdenum oxide cluster, {Mo_{132}} (formula: $[Mo^{VI}_{72}Mo^{V}_{60}O_{372}(CH_3COO)_{30}(H_2O)_{72}]^{42-}$), with systematically varied reaction parameters have been fully explored to determine the morphologies and concentration of products, reduction of metal centers, and chemical environments of the organic ligands. The growth of these clusters shows a typical sigmoid curve, suggesting a general multistep self-assembly mechanism for the formation of giant molecular clusters. The reaction starts with a lag phase period when partial Mo^{VI} centers of molybdate precursors are reduced to form {Mo^{V}_2(acetate)} structures under the coordination effect of the acetate groups. Once the concentration of {Mo^{V}_2(acetate)} reaches a critical value, it triggers the co-assembly of Mo^{V} and Mo^{VI} species into the giant clusters.

INTRODUCTION

The construction of giant molecular clusters, a group of monodispersed and well-defined nanoparticles, including nanocage, metal−organic polyhedra, and polyoxometalates (POMs), requires the precise manipulation of atoms and molecules in the self-assembly pathways.[1−5] However, the rational design of inorganic oxide clusters is still beyond our capacity because of the complexity of the self-assembly behavior of metal-oxo polyhedra, although the research on them has become a hot topic recently due to their seemingly limitless scope of practical and fundamental uses, including serving as catalysts, photoelectronic/magnetic materials, biologically active materials, and in the emergent fields of spintronics and quantum computing.[1,6−10]

Initiated and led by Müller and co-workers, the synthesis and structural characterization of protein-sized metal oxide clusters (2−6 nm) have generated great interest in the areas of physics, biology, chemistry, and materials science.[11,12] A templated-synthesis mechanism has been recently proposed and successfully explained the formation of several metal oxide clusters.[13−16] Small clusters and counterions are usually the

Received: June 8, 2016
Published: July 26, 2016

DOI: 10.1021/jacs.6b05882
J. Am. Chem. Soc. 2016, 138, 10623−10629

transient templates in the self-assembly of these clusters.[13−16] Nevertheless, a large numbers of clusters are actually synthesized upon simple reduction of the molybdenum precursors without the existence of templates although rare clusters, e.g., $\{Mo_{36}\}$, can form in solution without reduction.[12,17] It was stated as an empirical rule by Müller that, "upon increasing the size of [POMs], the charge density on the anion has to be kept approximately constant (which means increasing the overall charge) in order to keep the anion in growth as a soluble, nonhydrolyzing entity in solution."[12] Under the guidance of Müller, the reduction of metal centers, mainly Mo centers, was used as a general protocol to prepare giant POMs.[18−20] A template-based reduction-assisted growth theory has been proposed for the formation process of cluster $\{Mo_{154}\}$.[13] However, the critical role that the reducing agents play, as well as other reaction parameters in the formation process of these giant clusters, remains unclear. A general theory is urgently needed to fully understand the role that reduction plays in the self-assembly of these clusters to make rational design and synthesis possible for metal oxide clusters. Herein, a thorough understanding of the reduction-triggered self-assembly pathway is obtained based on simultaneous acquisition of information regarding intermittent product morphology, the location of ligands, and oxidation states/coordination environment of Mo centers in the synthesis of a 2.9 nm $\{Mo_{132}\}$ cluster (formula: $[Mo^{VI}_{72}Mo^{V}_{60}O_{372}(CH_3COO)_{30}(H_2O)_{72}]^{42-}$) (Figure 1).[21,22] The growth kinetics of giant POM clusters is, for the first time, revealed to be a multistep self-assembly process.

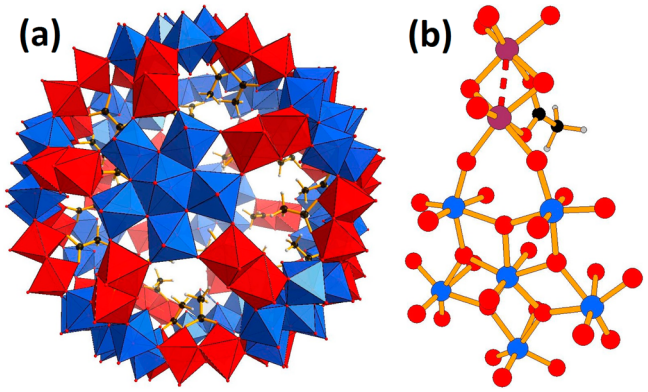

Figure 1. (a) Graphical representation of $\{Mo_{132}\}$ structure; (b) ball−stick model of the $\{(Mo^{VI})(Mo^{VI})_5\}$ unit connected to $\{(Mo^{V})_2(acetate)\}$ unit. Color code for polyhedron: blue, $Mo^{VI}O_6$ or $Mo^{VI}O_7$; red, $Mo^{V}O_6$. Color code for spheres: blue, Mo^{VI}; plum, Mo^{V}; red, O; black, C; gray, H.

EXPERIMENTAL SECTION

General Details. The reaction solution for UV−vis study was put in a 1 mm thick quartz cuvette for measurements. The UV−vis measurements were performed using a Varian Cary 5000 absorption spectrometer. The sample solutions for ^{1}H NMR studies were conducted in 5 mm NMR tubes. The measurements were done at 23 °C on a Varian VNMRS 500 MHz NMR spectrometer, operating at 499.7 MHz for proton, in D_2O. The synthesis of $\{Mo_{132}\}$ was carried out following previously well-documented protocols.[21] In a typical synthetic reaction, $(NH_4)_6Mo_7O_{24}\cdot 4H_2O$ (0.280 g, 0.227 mmol) and CH_3COONH_4 (0.625 g, 8.108 mmol) were dissolved in 12.50 mL of de-ionized (DI) water. Hydrazine sulfate ($N_2H_6SO_4$, 0.040 g, 0.307 mmol) was then added and the solution was stirred for 10 min. After that, 50% acetic acid solution (4.15 mL) was added. This reaction solution was monitored in real time and served as the reference for assessment of control parameters. To investigate the effect of the quantity of reducing agent employed, three substitutive doses of hydrazine sulfate, namely 0.083 (0.638 mmol), 0.013 (0.100 mmol), and 0.220 g (1.691 mmol), were used in the above synthetic reactions for comparison. For the study of the effect of different types of reducing agents, ascorbic acid (0.054 g, 0.307 mmol), iron powder (0.017 g, 0.304 mmol), and $SnCl_2\cdot 2H_2O$ (0.068 g, 0.301 mmol) were used to replace hydrazine sulfate in the synthetic reactions, respectively. In order to assess the effect of pH, 0, 1.5, 3, 4.5, 7.5, and 12 mL of glacial acetic acid, 0.50 mL of concentrated H_2SO_4 in 4 mL of H_2O, 1.50 mL of concentrated HCl in 3 mL of H_2O were used instead of 4.15 mL of 50% acetic acid solution in the reactions, respectively. For the evaluation on the role of ligands, a reaction solution with pH tuned to ∼3 through concentrated HCl was employed to compare with the case of 4.15 mL of 50% acetic acid.

Synthesis of $\{Mo_{248}\}$. According to a previous literature procedure, this cluster was synthesized by dissolving 3 g of Na_2MoO_4 (14.569 mmol) in 45 mL of H_2O. The solution was then acidified with 2.5 mL of 32% HCl with stirring. After that, 1.2 mL of 0.5 M ascorbic acid solution was added and the solution allowed to stand for crystallization.[23] In our studies, hydrazine sulfate instead of ascorbic acid was used in the synthetic reactions. The solution was prepared by dissolving 0.6 g of Na_2MoO_4 (2.914 mmol) in 9 mL of H_2O, and then acidified with 0.5 mL of 32% HCl solution under stirring. Then 0.08 g of hydrazine sulfate (0.615 mmol) was added to the reaction solution. The obtained solution was used for SAXS monitoring.

Synthesis of Na·$\{Mo_{132}\}$ and Li·$\{Mo_{132}\}$·Na·$\{Mo_{132}\}$. $Na_2MoO_4\cdot 2H_2O$ (0.152 g, 0.628 mmol) and CH_3COONa (0.266 g, 3.243 mmol) were dissolved in 5 mL of DI water. Hydrazine sulfate ($N_2H_6SO_4$, 0.016 g, 0.123 mmol) was then added and the solution stirred for 10 min. After that, 50% acetic acid solution (1.66 mL) was added. Yield: 0.024 g (19% based on Mo). **Li·$\{Mo_{132}\}$**: Li_2MoO_4 (0.110 g, 0.633 mmol) and CH_3COOLi (0.214 g, 3.243 mmol) were dissolved in 5 mL of DI water. Hydrazine sulfate ($N_2H_6SO_4$, 0.016 g, 0.123 mmol) was then added, and the solution was stirred for 10 min. After that, 50% acetic acid solution (1.66 mL) was added. Yield: 0.024 g (19% based on Mo). Crystals of the two products can be obtained by slow evaporation of the solvents. For ^{1}H NMR study, d_4-acetic acid and D_2O were used instead of acetic acid and water in the synthesis of Na·$\{Mo_{132}\}$.

SAXS. The SAXS experiments were performed at the 12-ID-C station with X-ray energy of 20 keV at the Advanced Photon Source (APS) of the Argonne National Laboratory (ANL). The sample-to-detector distance was about 2 m. A Pilatus detector (Dectris Ltd.) was used to acquire images with typical exposure times in the range of 0.1 to 1.0 s for a single measurement. The sample solutions were placed in quartz capillaries for all the measurements. For each of the sample measurements, SAXS measurements of corresponding solvents were also carried out for background reduction. The theoretical SAXS function of the sample solution assuming the corresponding crystal structure is calculated with the following equation:

$$I(q) = \sum_i \sum_{j\neq i} b_i b_j \frac{\sin(qr_{ij})}{qr_{ij}}$$

where r_{ij} represents the distance between atoms i and j, b denotes the respective atom's X-ray scattering length approximated by its number of electrons, and the summations run over all the atoms in the crystal structure. It is important to note that this computation method is reasonable because the X-ray scattering length (equivalently electron number) of Mo in the solute is exceedingly higher than that of the solvent rendering the latter negligible in the calculation.

XANES. Mo K-edge (19.900−20.100 keV) XANES spectra were collected simultaneously with SAXS data in 12-ID-C of APS in ANL at room temperature in fluorescence mode using a vortex Si-drift detector. The spectra were energy calibrated with respect to the first inflection point in the XANES spectra of a Mo metal foil (20.000

DOI: 10.1021/jacs.6b05882
J. Am. Chem. Soc. 2016, 138, 10623−10629

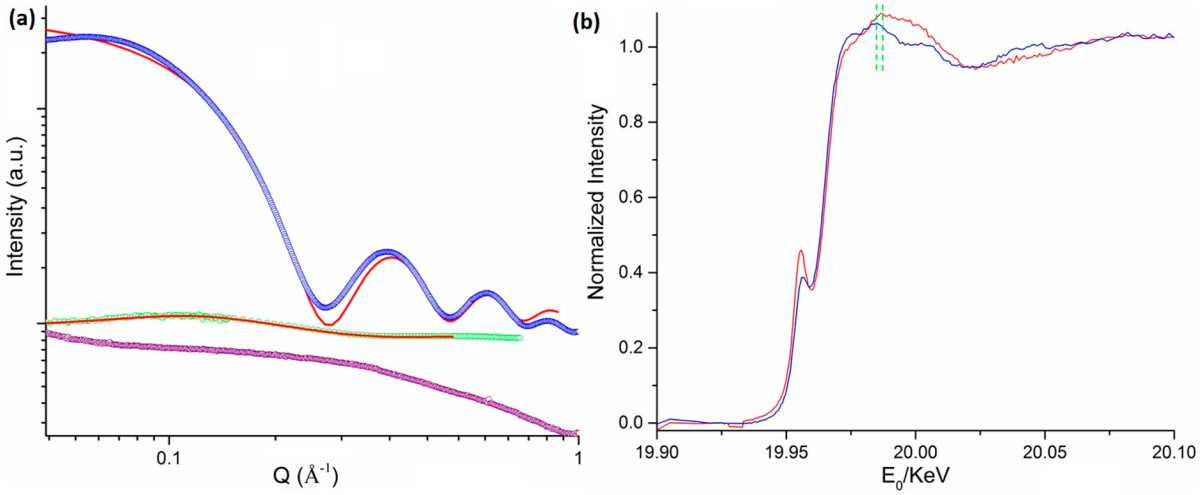

Figure 2. (a) SAXS (blue circle) and SANS (green circle) data of $\{Mo_{132}\}$ solutions and the fitted curves (red) generated from the crystal structures and SAXS data of $(NH_4)_6Mo_7O_{24}$ (purple circle). (b) XANES results of $\{Mo_{132}\}$ (red) solutions and $(NH_4)_6Mo_7O_{24}$ (blue).

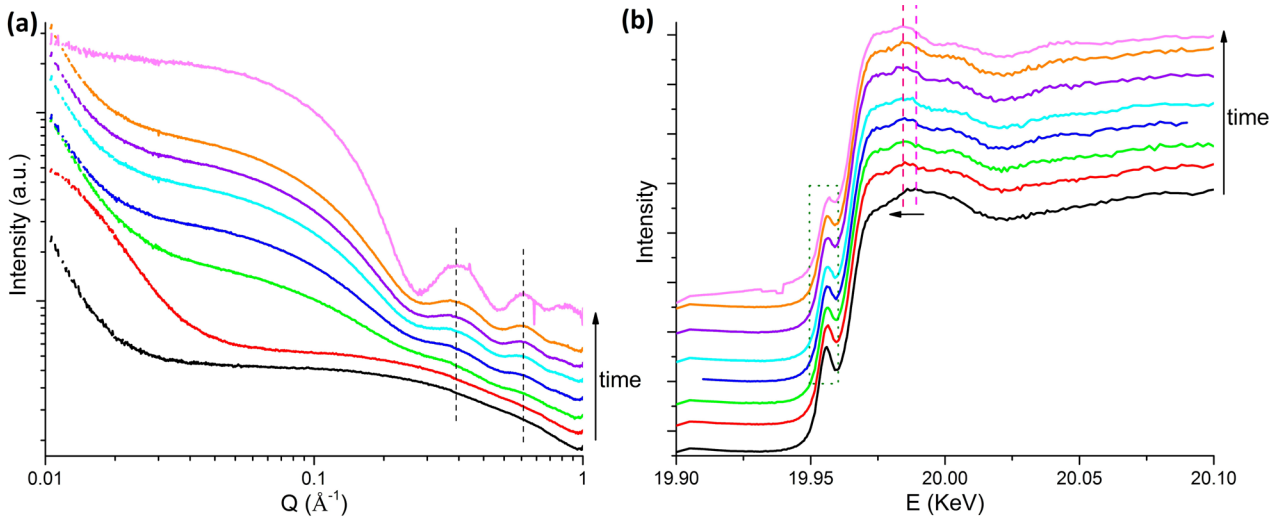

Figure 3. (a) Time-resolved SAXS and (b) XANES studies of the synthetic reactions of $\{Mo_{132}\}$ from reaction time 0 to 19 h.

keV). The obtained data reduction and analysis were performed with PyMca software following standard procedure.[24]

SANS. The solution for SANS study was prepared by dissolving 100 mg of $\{Mo_{132}\}$ crystalline samples in 1 mL of D_2O. The SANS spectrum $I(q)$ can be factorized into form factor $P(q)$ and structure factor $S(q)$ as following:[25]

$$I(q) = AP(q)S(q) + I_{inc}$$

where A represents scattering contrast and I_{inc} accounts for incoherent background. The form factor encodes the intra-POM scattering length density (SLD) distribution, for which a core−shell type structure is used. The choice of this model is inspired by the recent study that suggests the water molecule can penetrate into the inside of POM and more importantly adopt different packing pattern comparing to their bulk condition thereby yielding coherent neutron scattering contrast.[26] The presence of nontrivial structure factor is evidenced by the strong interaction peak at q = 0.1 Å^{-1} clearly resulting from screened Coulomb repulsion among charged POMs at higher concentration in comparison to the sample for SAXS measurement. The structure factor is solved by coupling Ornstein−Zernike equation with hypernetted-chain (HNC) closure.[27] Within this framework, we carried out model fitting with least-squares optimization method and obtained the scattering length density of the core structure, based on which number of water molecule inside POM is estimated.[28] This estimation is found to be larger than the study but smaller if the water molecules inside POM are in bulk condition.[26] This result will appear in future publications.

RESULTS AND DISCUSSION

SAXS, SANS, and XANES Studies of $\{Mo_{132}\}$ Compounds in Solutions. The crystalline samples of $\{Mo_{132}\}$ were synthesized according to previous literature procedures.[21] Their aqueous solutions as well as the solution of the molybdenum precursor in the synthetic reaction, $(NH_4)_6Mo_7O_{24}{\cdot}4H_2O$, are prepared and considered as standard samples for initial small-angle X-ray scattering (SAXS) and X-ray absorption near edge structure (XANES) studies. The SAXS spectrum of $\{Mo_{132}\}$ standard samples is quite different from that of the precursor (Figure 2a). It is evident that the SAXS measurement on the $\{Mo_{132}\}$ standard sample agrees remarkably well with the theoretical scattering function computed from its single crystal structures. Moreover, analysis on small angle neutron scattering (SANS) spectrum of $\{Mo_{132}\}$'s D_2O solution further confirms that the acetate ligands indeed locate inside the inorganic capsule framework (Figures 1 and 2a). Hence small angle scattering (SAS) results

DOI: 10.1021/jacs.6b05882
J. Am. Chem. Soc. 2016, 138, 10623−10629

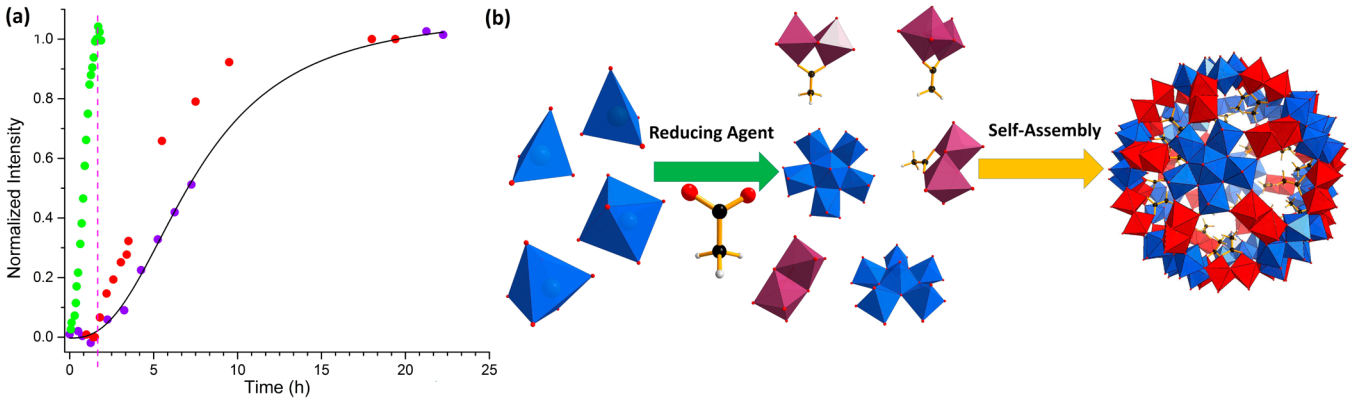

Figure 4. (a) Kinetic data from UV−vis (green dots), SAXS (red dots), and ^{1}H NMR (purple dots) monitoring results. The ^{1}H NMR data fits quite well with standard sigmoid curve (Hill equation in Origin fitting package). (b) Graphical representation of the formation process of {Mo_{132}} clusters.

indicate that the molecules of {Mo_{132}} are stable and maintain the same morphologies as their crystal counterparts in solutions. Meanwhile, XANES studies of solution samples of the standard and the precursor provide information on the oxidation state and coordination environment of the Mo centers (Figure 2b). The two samples show qualitative resemblance in XANES results, both of which reflect the domination of a typical coordination environment of six-coordinate Mo atoms.[29,30] A red shift of the post-edge peak can be observed between $(NH_4)_6Mo_7O_{24}$ and standard samples of {Mo_{132}} (green vertical dashed lines in Figure 2b). It is clear that the features in XANES move progressively to higher energy as the Mo oxidation state is raised, which is consistent with the fact that partial Mo centers in the standard {Mo_{132}} sample have been reduced from Mo^{VI} to Mo^{V}.[21,31,32] It is suggested from previous work that Mo (VI) complexes having Mo═O bonds show the pre-edge peak which is assigned to a 1s-4d transition, and that the peak intensity increases with the number of terminal oxygens per Mo center, *n*.[29,30] Indeed, $Mo_7O_{24}^{6-}$ shows higher intensities at pre-edge peak position (19.956 keV) than the giant cluster does. To our understanding, in the condensation process, the terminal oxo ligands of the precursor transform into bridge oxo ligands to connect them into larger clusters.

Time-Resolved SAXS and XANES Studies of the Synthetic Reactions of {Mo_{132}}. Typical reactions for the synthesis of {Mo_{132}} ({Mo_{132}} denotes the cluster with ammonium counterions unless otherwise noted) are monitored by synchrotron-based SAXS and XANES simultaneously. The featured oscillation peaks at 0.3430 and 0.5950 $Å^{-1}$ (labeled by the black dashed lines in Figure 3a) are used as indications for the formation of target cluster products. SAXS studies indicate that the formation of the clusters can be observed within ∼2 h (green curve), suggesting that the clusters form in the reaction solution, not during the crystallization process (Figure 3a). The intensities of the oscillation peak increase in amplitude without any shift of the oscillation peaks as the reactions progress. This is strong evidence indicating the formation of more and more clusters. XANES studies of the synthetic reactions show a gradual red-shift of post-edge peak (labeled by the purple and red dashed lines in Figure 3b) and a decrease of the pre-edge peak (highlighted by the rectangle outlined in green dots), indicating the reduction of Mo centers and the nucleation of Mo centers during the reaction process (Figure 3b).[29−32]

Growth Kinetics of the Clusters. Quantitative examination of the reaction solution of {Mo_{132}} by UV−vis, ^{1}H NMR, and SAXS is able to provide the first kinetic study of the formation process of giant POM clusters. Due to strong interaction between the anionic clusters and ammonium, the {Mo_{132}} clusters can easily crystallize during the reaction to synthesize NH_4·{Mo_{132}} even though the reaction has not reached the equilibrium state.[21] It is observed that the sodium form of {Mo_{132}} can only crystallize out from the solutions by slow evaporation of the solvents. Therefore, in order to capture a complete view of the kinetics, the synthetic reaction of Na·{Mo_{132}} ({Mo_{132}} with sodium as counterions) is used for studying the growth of reduction-triggered formation of giant POM clusters. The intensities of the first oscillation peak in SAXS results were used to quantitatively describe the kinetics of the growth of the inorganic shell of the clusters (Figure 4a and Figure S1 in Supporting Information). In ^{1}H NMR measurements, the confined immobilized acetate groups inside the {Mo_{132}} clusters show distinct peaks at ∼0.5 ppm to their free counterparts in solutions, whose chemical shift is at ∼1.8 ppm.[33] The peaks corresponding to the confined acetate groups were observed to increase gradually during the reaction process, suggesting that the concentration of immobilized acetate increases (Figure S2 in Supporting Information). Quantitative analysis of the ^{1}H NMR data shows a typical sigmoid curve, which is coincident with the SAXS monitoring results of the same reactions, suggesting that the growth of the inorganic shell of the clusters is concomitant with the encapsulation and immobilization of acetate groups inside the clusters (Figure 4a). This sigmoidal kinetic curve is typical for the synthesis of product or self-assembly process by any multistep reaction. Suggested by the kinetic curves of SAXS and ^{1}H NMR results, the first 2 h period in the reaction, marked by the pink dashed line, is indicated as the lag phase period in the growth of {Mo_{132}} clusters. Interestingly, UV−vis monitoring of the characteristic absorption peak of the {Mo^{V}_2} dimer structure at ∼450 nm during the reaction process indicates that such dimer species forms immediately as the reduction reaction starts and reaches the highest concentration at 1.9 h (Figure 4a). A comprehensive three-stage kinetic view can be summarized from the above studies (Figure 4b). (1) Initial lag phase: in the first 2 h of the reaction, partial Mo^{VI} centers of molybdate precursors were reduced and formed {Mo^{V}_2(acetate)} structures under the coordination effect of acetate groups. (2) Rapid assembly: the concentration of {Mo^{V}_2(acetate)} reached a critical value to trigger the assembly of Mo^{V} and Mo^{VI} species into {Mo_{132}} clusters.[34] (3) Asymptotic phase: the self-

DOI: 10.1021/jacs.6b05882
J. Am. Chem. Soc. 2016, 138, 10623−10629

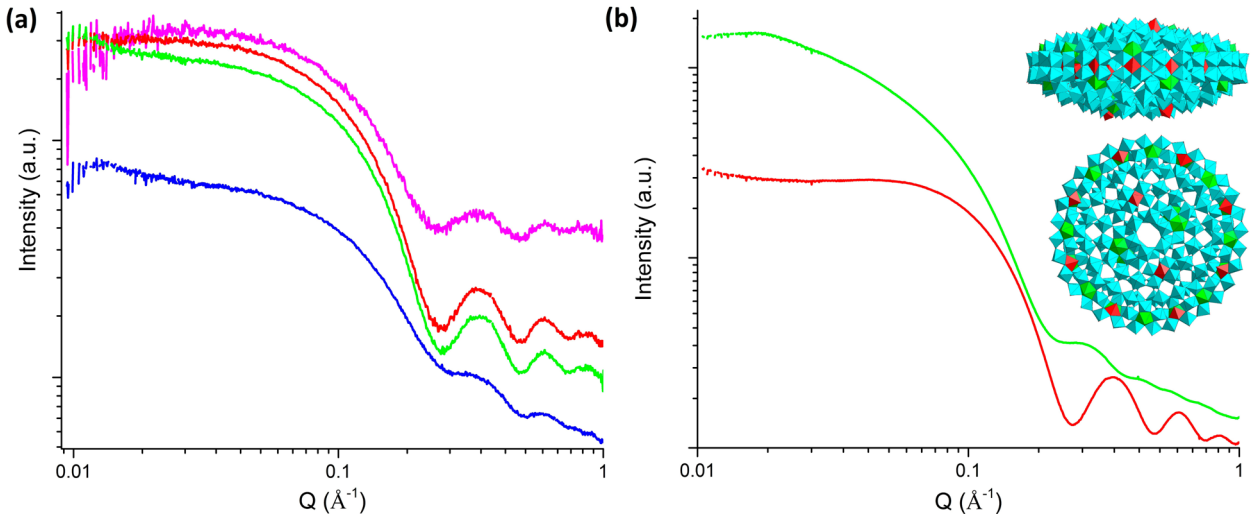

Figure 5. (a) SAXS results of synthetic reactions of {Mo_{132}} with different amount of reducing agents (6.0 mmol, blue; 18.3 mmol, green; 37.8 mmol, red; 100.6 mmol, magenta). (b) SAXS results of synthetic reaction of {Mo_{132}} with ascorbic acid as reducing agents (red) and synthetic reaction of {Mo_{248}} with hydrazine sulfate as reducing agents. Inset: graphic representation of side and top views of {Mo_{248}} cluster.

assembly rate slows down because of the consumption of {Mo^{V}_{2}(acetate)} as the reaction progresses.

Effect of Reducing Agents. The critical role of reducing agents has been clarified by monitoring the synthetic reactions of {Mo_{132}} clusters as a function of both the amount of reducing agent (hydrazine sulfate), and the type of reducing agent. The synthetic reactions for {Mo_{132}} with hydrazine sulfate concentrations of 6.0, 18.3, 37.8, and 100.6 mM, respectively, and Mo^{VI} concentrations of 95.4 mM were carried out and monitored by SAXS. The monitoring experiments indicate that the target clusters can still be observed in all the synthetic reactions, however, with different concentrations. The intensity of the first oscillation peak at 0.3430 Å^{-1} in the scattering curve is used as the qualitative index for the concentration of formed {Mo_{132}} clusters in solution. It is suggested that the reactions with medium reducing agent concentrations (18.3 and 37.8 mM) achieve higher product concentrations than the other two reactions (Figure 5a). The formation of large clusters requires the coexistence of Mo^{V} and Mo^{VI} centers in an optimized ratio (for {Mo_{132}}, this ratio is 5:6).[35] The Mo^{VI} centers are responsible for the construction of {(Mo)$(Mo)_5$} units in the framework of POM clusters while Mo^{V} dimer units play the roles of linker that binds the units to 3D structures (Figure 1). Ideally, based on the stoichiometry of the reaction, 9.2 mM would be the optimum concentration of hydrazine sulfate to achieve highest yield. However, considering the reaction efficiency and side reactions with air, the ratio could shift. It is indicated from the experiment results that varying the reducing agent concentrations to either too low (<6.0 mM) or too high (>100.6 mM) will lower the yields of the reactions.

Although it is believed that the nature of the reducing agent could be an important parameter for synthesizing different types of giant clusters, our study suggests that the nature of the reducing agent is not critical in the formation of {Mo_{132}}.[36,37] Herein, several common reducing agents used for giant POM synthesis, specifically ascorbic acid, Fe powder, and $SnCl_2$, instead of hydrazine sulfate, are used in the {Mo_{132}} synthetic reaction. As suggested from the SAXS studies of the reaction solutions, the formation of {Mo_{132}} clusters can still be observed in all these reactions (Figure 5b and Figures S3−S5 in Supporting Information). On the other hand, hydrazide sulfate is used to replace the original reducing agent, ascorbic acid, in the synthetic reaction of another giant cluster, {Mo_{248}} and SAXS monitoring results indicate that {Mo_{248}} is the major species formed in the reaction solution (Figure 5b).[23]

The Role the Buffer Plays in the Formation of Clusters. The synthesis of {Mo_{132}} clusters is carried out in buffers of carboxylic acids.[21,38,39] The roles of the buffer can be divided into two parts: pH and ligand effect. The synthetic reactions were further carried out in buffers with pH ranging from 0 to 6 by adding strong acid or acetic acid. Our experimental results indicate that the formation of {Mo_{132}} can only be observed in the pH range of 3.0−4.1 (Figures S6 and S7 in Supporting Information). That is consistent with previous research of Müller and co-workers on the synthesis of Mo blue species and {Mo_{132}}.[40] More experiments have been done by using hydrochloric acid instead of acetic acid to lower the solution pH to ∼3.0. Mo blue species instead of {Mo_{132}} form in the reaction solutions (Figure S8 in Supporting Information). Without the excessive amount of acetate groups, the {Mo_{132}} cluster is not the favored product in the reactions. Therefore, the formation of edge-sharing {Mo^{V}_{2}} requires both the optimal buffer pH for acid-catalyzed condensation reaction of molybdate precursors and the stabilization effect from the coordination of the acetate ligands.[34,35]

The cations in the buffer have also been explored for their possible effect in the synthesis of {Mo_{132}}. Cations have been experimentally and theoretically confirmed to play significant roles in templating the self-assembly of uranyl-peroxide nanoclusters.[16,41] It was concluded in the previous literature that the curvature of the nanocluster is enhanced by cation coordination, which is suggested to be the driving force for the self-assembly process.[16] However, {Mo_{132}} clusters, confirmed by *in situ* SAXS and NMR studies, are still the products in the reactions with sodium or lithium as the cations in the reaction solutions (Figures S9−S11 in Supporting Information). Unlike the uranyl-peroxide nanoclusters, the curvature of the {Mo_{132}} cluster is mainly determined by the ligand coordination to the Mo^{V} dimer structure instead of the cation coordination (Figure 1).

DOI: 10.1021/jacs.6b05882
J. Am. Chem. Soc. 2016, 138, 10623−10629

CONCLUSION

A reducing agent-triggered formation process of $\{Mo_{132}\}$ has been fully explored, and the kinetics of giant POMs synthesis has been, for the first time, uncovered to be a typical sigmoid-shape multistep assembly process. Unexpectedly, the type of reducing agent and the counterions in the reaction buffer was shown to have limited effect in the formation of giant clusters. The quantity of the reducing agent plays a decisive role in controlling the yield of the target clusters. For a given level of reducing agent, the pH and the organic ligands of the buffer are the two key factors in the formation process of $\{Mo_{132}\}$ clusters. Our studies are instructive in the design and synthesis of giant POM clusters via reduction. This protocol can also be used to optimize the synthesis of POM clusters and search for new materials.

ASSOCIATED CONTENT

Supporting Information

The Supporting Information is available free of charge on the ACS Publications website at DOI: 10.1021/jacs.6b05882.

Figures S1−S12; discussions on the synthetic reaction of $\{Mo_{248}\}$ using hydrazine sulfate instead of ascorbic acid as reducing agent, pH effect, Mo blue species formed in synthetic reactions using HCl to bring down the pH to ∼3, and counterion-dependent crystallization behaviors; and SANS instrumental details (PDF)

AUTHOR INFORMATION

Corresponding Author

*yinp@ornl.gov

Notes

The authors declare no competing financial interest.

ACKNOWLEDGMENTS

P.Y. is grateful for the support of the Clifford G. Shull Fellowship from Neutron Sciences Directorate of Oak Ridge National Laboratory. The research performed in BL-6 (EQ-SANS) at ORNL's Spallation Neutron Source was sponsored by the Scientific User Facilities Division, Office of Basic Energy Sciences, U.S. Department of Energy (DOE). The sample preparation and initial SAXS study in the X-ray lab were conducted at the Center for Nanophase Materials Sciences, which is a DOE Office of Science User Facility. Oak Ridge National Laboratory is supported by the Office of Science of the U.S. Department of Energy under Contract No. DE-AC05-00OR22725. The synchrotron-based SAXS and XANES studies carried out in 12-ID-C used resources of the Advanced Photon Source, a U.S. Department of Energy Office of Science User Facility operated for the DOE Office of Science by Argonne National Laboratory under Contract No. DE-AC02-06CH11357. The authors also thank the Institut Laue Langevin for neutron beamtime. The helpful discussions from Dr. Anibal J. Ramirez-Cuesta and Prof. Ira A. Weinstock are also acknowledged here.

REFERENCES

(1) Cronin, L.; Müller, A. *Chem. Soc. Rev.* **2012**, *41*, 7333.
(2) Chakrabarty, R.; Mukherjee, P. S.; Stang, P. J. *Chem. Rev.* **2011**, *111*, 6810.
(3) Ballester, P.; Fujita, M.; Rebek, J. *Chem. Soc. Rev.* **2015**, *44*, 392.
(4) Müller, A.; Roy, S. In *The Chemistry of Nanomaterials: Synthesis, Properties and Applications*; Rao, C. N. R., Müller, A., Cheetham, A. K., Eds.; Wiley-VCH Verlag GmbH & Co. KGaA: Weinheim, 2005; Vol. *1*, p 452.
(5) Jones, J. T. A.; Hasell, T.; Wu, X.; Bacsa, J.; Jelfs, K. E.; Schmidtmann, M.; Chong, S. Y.; Adams, D. J.; Trewin, A.; Schiffman, F.; Cora, F.; Slater, B.; Steiner, A.; Day, G. M.; Cooper, A. I. *Nature* **2011**, *474*, 367.
(6) Long, D.-L.; Burkholder, E.; Cronin, L. *Chem. Soc. Rev.* **2007**, *36*, 105.
(7) Hill, C. L. *Chem. Rev.* **1998**, *98*, 1.
(8) Fleming, C.; Long, D.-L.; McMillan, N.; Johnston, J.; Bovet, N.; Dhanak, V.; Gadegaard, N.; Kogerler, P.; Cronin, L.; Kadodwala, M. *Nat. Nanotechnol.* **2008**, *3*, 289.
(9) Busche, C.; Vila-Nadal, L.; Yan, J.; Miras, H. N.; Long, D.-L.; Georgiev, V. P.; Asenov, A.; Pedersen, R. H.; Gadegaard, N.; Mirza, M. M.; Paul, D. J.; Poblet, J. M.; Cronin, L. *Nature* **2014**, *515*, 545.
(10) Bertaina, S.; Gambarelli, S.; Mitra, T.; Tsukerblat, B.; Muller, A.; Barbara, B. *Nature* **2008**, *453*, 203.
(11) Müller, A.; Gouzerh, P. *Chem. Soc. Rev.* **2012**, *41*, 7431.
(12) Müller, A.; Peters, F.; Pope, M. T.; Gatteschi, D. *Chem. Rev.* **1998**, *98*, 239.
(13) Miras, H. N.; Cooper, G. J. T.; Long, D.-L.; Bögge, H.; Müller, A.; Streb, C.; Cronin, L. *Science* **2010**, *327*, 72.
(14) Qiu, J.; Ling, J.; Sui, A.; Szymanowski, J. E. S.; Simonetti, A.; Burns, P. C. *J. Am. Chem. Soc.* **2012**, *134*, 1810.
(15) Yin, P.; Wu, B.; Mamontov, E.; Daemen, L. L.; Cheng, Y.; Li, T.; Seifert, S.; Hong, K.; Bonnesen, P. V.; Keum, J. K.; Ramirez-Cuesta, A. J. *J. Am. Chem. Soc.* **2016**, *138*, 2638.
(16) Miró, P.; Pierrefixe, S.; Gicquel, M.; Gil, A.; Bo, C. *J. Am. Chem. Soc.* **2010**, *132*, 17787.
(17) Paulat-Boschen, I. *J. Chem. Soc., Chem. Commun.* **1979**, 780.
(18) Jiang, C.-C.; Wei, Y.-G.; Liu, Q.; Zhang, S.-W.; Shao, M.-C.; Tang, Y.-Q. *Chem. Commun.* **1998**, 1937.
(19) Yamase, T.; Prokop, P. V. *Angew. Chem., Int. Ed.* **2002**, *41*, 466.
(20) Nakamura, I.; Miras, H. N.; Fujiwara, A.; Fujibayashi, M.; Song, Y.-F.; Cronin, L.; Tsunashima, R. *J. Am. Chem. Soc.* **2015**, *137*, 6524.
(21) Müller, A.; Krickemeyer, E.; Bögge, H.; Schmidtmann, M.; Peters, F. *Angew. Chem., Int. Ed.* **1998**, *37*, 3359.
(22) Müller, A.; Gouzerh, P. *Chem. - Eur. J.* **2014**, *20*, 4862.
(23) Müller, A.; Shah, S. Q. N.; Bogge, H.; Schmidtmann, M. *Nature* **1999**, *397*, 48.
(24) Solé, V. A.; Papillon, E.; Cotte, M.; Walter, P.; Susini, J. *Spectrochim. Acta, Part B* **2007**, *62*, 63.
(25) Chen, S.-H. *Annu. Rev. Phys. Chem.* **1986**, *37*, 351.
(26) Müller, A.; Garai, S.; Schäffer, C.; Merca, A.; Bögge, H.; Al-Karawi, A. J. M.; Prasad, T. K. *Chem. - Eur. J.* **2014**, *20*, 6561.
(27) Hansen, J.-P.; McDonald, I. R. *Theory of Simple Liquids*; Academic Press: Burlington, 2006; p 341.
(28) In *Neutrons, X-rays and Light: Scattering Methods Applied to Soft Condensed Matter*; Zemb, T., Lindner, P., Eds.; Elsevier: Amsterdam, 2002.
(29) Yokoi, K.; Matsubayashi, N.; Miyanaga, T.; Watanabe, I.; Murata, K.; Ikeda, S. *Chem. Lett.* **1987**, *16*, 1453.
(30) Yokoi, K.; Matsubayashi, N.; Miyanaga, T.; Watanabe, I.; Ikeda, S. *Polyhedron* **1993**, *12*, 911.
(31) Cramer, S. P.; Eidem, P. K.; Paffett, M. T.; Winkler, J. R.; Dori, Z.; Gray, H. B. *J. Am. Chem. Soc.* **1983**, *105*, 799.
(32) Cramer, S. P.; Hodgson, K. O.; Gillum, W. O.; Mortenson, L. E. *J. Am. Chem. Soc.* **1978**, *100*, 3398.
(33) Ziv, A.; Grego, A.; Kopilevich, S.; Zeiri, L.; Miro, P.; Bo, C.; Müller, A.; Weinstock, I. A. *J. Am. Chem. Soc.* **2009**, *131*, 6380.
(34) Schaffer, C.; Todea, A. M.; Gouzerh, P.; Muller, A. *Chem. Commun.* **2012**, *48*, 350.
(35) Botar, B.; Ellern, A.; Kögerler, P. *Dalton Trans.* **2012**, *41*, 8951.
(36) Müller, A.; Roy, S. *Coord. Chem. Rev.* **2003**, *245*, 153.
(37) Müller, A.; Kögerler, P. *Coord. Chem. Rev.* **1999**, *182*, 3.
(38) Schäffer, C.; Bögge, H.; Merca, A.; Weinstock, I. A.; Rehder, D.; Haupt, E. T. K.; Müller, A. *Angew. Chem., Int. Ed.* **2009**, *48*, 8051.
(39) Schäffer, C.; Todea, A. M.; Bögge, H.; Petina, O. A.; Rehder, D.; Haupt, E. T. K.; Müller, A. *Chem. - Eur. J.* **2011**, *17*, 9634.

DOI: 10.1021/jacs.6b05882
J. Am. Chem. Soc. 2016, 138, 10623−10629

(40) Müller, A.; Das, K.; Krickemyer, E.; Kuhlmann, C. In *Inorganic synthesis*; Shapley, J. R., Ed.; John Wiley & Sons, Inc.: Hoboken, NJ, 2004; Vol. *34*, p 191.
(41) Qiu, J.; Vlaisavljevich, B.; Jouffret, L.; Nguyen, K.; Szymanowski, J. E. S.; Gagliardi, L.; Burns, P. C. *Inorg. Chem.* **2015**, *54*, 4445.

DOI: 10.1021/jacs.6b05882
J. Am. Chem. Soc. 2016, 138, 10623−10629